

RECENT ADVANCES IN MODELLING THE OHAAKI GEOTHERMAL FIELD

E.K. Clearwater¹, M.J. O'Sullivan¹, W.I. Mannington², J.A. Newson² and K. Brockbank²

¹Department of Engineering Science, University of Auckland, Private Bag 92019, Auckland 1142, New Zealand

²Wairakei Power Station, Contact Energy, State Highway 1, Private Bag 2001, Taupo 3352, New Zealand

ecle011@aucklanduni.ac.nz

Keywords: *Ohaaki, Geothermal, Modelling, TOUGH2.*

ABSTRACT

A sequence of three-dimensional numerical models, of increasing complexity, of the Ohaaki geothermal system have been developed at the University of Auckland in collaboration with Contact Energy Ltd (CEL) and its predecessors. A report on one of the most recent versions of these models (called here Model 2012) formed part of the application for the re-consenting of the Ohaaki Geothermal Power Project, approved at an RMA hearing in 2013. The current paper summarises the report on the 2012 model and discusses improvements to the model that have been made since 2012.

1. INTRODUCTION

The Ohaaki geothermal system lies on the eastern margin of the Taupo Volcanic Zone (TVZ). Drilling commenced at Ohaaki in 1965, with a total of 44 wells drilled between 1966 and 1984. There was an extended period of well testing and recovery up to 1988, when the Ohaaki Geothermal Power Project (OGPP) was commissioned (Lee and Bacon, 2000; Clotworthy *et al.*, 1995; Carey *et al.*, 2013). More than 65 wells have now been drilled in the area.

A sequence of numerical models of the Ohaaki system has been set up by O'Sullivan and co-workers (e.g. Blakeley *et al.*, 1983; Newson and O'Sullivan, 2001; Zarrouk and O'Sullivan, 2006; Clearwater *et al.*, 2011). As computer hardware and software has improved these models have increased in complexity and evolved into the large three dimensional models described here.

Two computer models of the Ohaaki geothermal system are discussed in the present paper. The first is the Model 2012, which has 22816 computational grid blocks and was used to generate the results reported to the 2013 RMA hearing on the re-consenting of the OGPP (O'Sullivan and Clearwater, 2013). The second is Model 2014 which has 45250 grid blocks and was developed during 2013/2014. The changes made to the model are related to our strategy of continuous model updating and improvement and partly related to issues that arose out of the 2013 RMA hearing. In particular we decided that it was necessary to improve the accuracy of the representation of shallow pressures in our model so that they could be used to make predictions about future subsidence at Ohaaki.

2. OHAAKI GEOTHERMAL SYSTEM

The Waikato River bisects the Ohaaki system, dividing it into the West Bank and East Bank areas (see Figure 1). Ohaaki (along with the other systems within the TVZ) is a high temperature liquid dominated convective system but is unusual in having a large content of gas (CO₂). There are two separate upflow zones for each of the East and West Banks, with deep temperatures in excess of 300°C (Hedenquist, 1990). A more detailed description of the

Ohaaki geothermal system can be found in Hedenquist, 1990 and Carey *et al.*, 2013.

The basement of the Ohaaki system is a pre-volcanic greywacke which down-faults to the north-west. This is overlain by a volcaniclastic sequence interspersed with dacitic and rhyolitic volcanic domes and flows (see Wood *et al.*, 2001; Rae *et al.*, 2007 and Carey *et al.*, 2013). The two main production units are the Waiora formation at depths of 400 to 1200m field wide, and the Tahorakuri formation on the West Bank below depths of 1500m (see Chapter 8 : Reservoir Engineering, in Carey *et al.*, 2013).

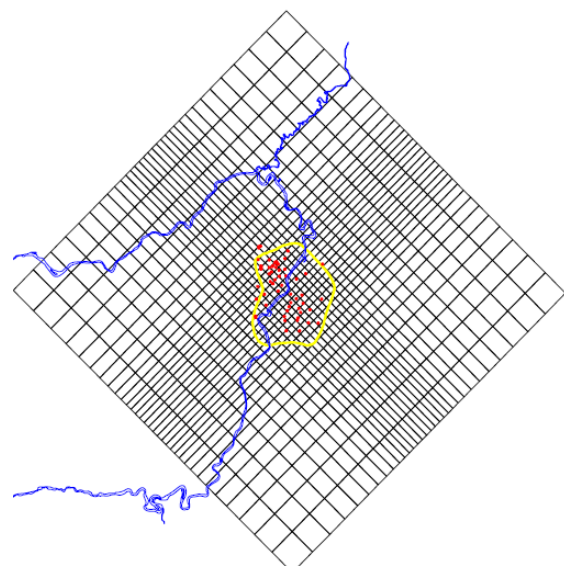


Figure 1: Plan view of the Ohaaki model grid. The blue line is the Waikato River, the yellow line the resistivity boundary (Risk *et al.*, 1970), and the red dots show the wells.

3. OHAAKI GEOTHERMAL POWER PROJECT

The plant commissioned in 1988 had a capacity of 116MWe and during the first 5 years of production, generation was maintained at ~100MWe. In 1993 the available steam began to decline. A deep drilling program was undertaken in 1995 which identified high temperatures and permeability in the deep volcanic formations underlying the West Bank (Lee and Bacon, 2000). This was relatively successful, however the steam supply continued to decline. A second deep drilling program also focused on the West Bank was undertaken in 2005-2007 (Rae *et al.*, 2007; Carey *et al.*, 2013) allowing generation output to be maintained at about 60MWe. A plot of annual electricity output (supplied by CEL) is shown in Figure 2.

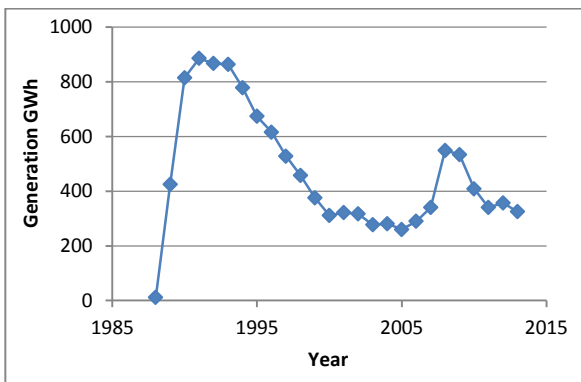


Figure 2: Annual electricity output from Ohaaki

3. RESERVOIR MODEL

3.1 Grid structure

The grid, whose plan view is shown in Figure 1, was first used in the model described in Clearwater *et al.*, (2011). The same horizontal grid structure has been retained for Model 2012 and Model 2014. The difference between all these models is in the layer structure which has become finer over time.

Hence, in Model 2012 there are 23 layers whereas in Model 2014 there are 57 layers (see Figure 3). In both models the layer structure below -190 mRL is the same but above this Model 2014 has finer layers. The finest section of the layer structure of Model 2014 is at the estimated location of the water table; where there are 6 x 10 m layers. Above and below these, there are several 20 m thick layers.

3.2 Boundary conditions

A change of the top boundary conditions for Model 2014 was introduced in order to allow accurate tracking of the movement of the water table and to better represent shallow pressure changes, particularly those that may be responsible for ground subsidence. This change is in addition to the refined layer structure which was also designed to allow more accurate representation of the water table.

The top of Model 2012 was set at the water table (interpolated from field data) and the temperature and pressure there are fixed at atmospheric conditions – a temperature of 10°C, pressure of 1bar. This type of boundary condition is a reasonable approximation if the position of the water table does not vary too much during production, but it may not be valid for Ohaaki as there is some evidence that shallow pressures have changed over time (Carey *et al.*, 2013).

Therefore for Model 2014 it was decided to improve the representation of the shallow zone and the movement of the water table by extending the model up to the ground surface. Topographical data was interpolated with a smooth surface which was used to calculate the top elevation for each column in the model. Then the top surface was fixed at atmospheric conditions of 15°C, a total pressure of 1 bar and a partial pressure of CO₂ of 0.9962 bar, giving a partial pressure of water vapour corresponding to 15°C. In addition, infiltration of rainfall was included at the top of the model corresponding to an annual average rain fall of 1325mm/yr (Carey *et al.*, 2013). The position of the water table is determined by a balance between the shallow

permeability and the infiltration rate of rainfall. Calibration of the water table position led to an infiltration rate of 10%.

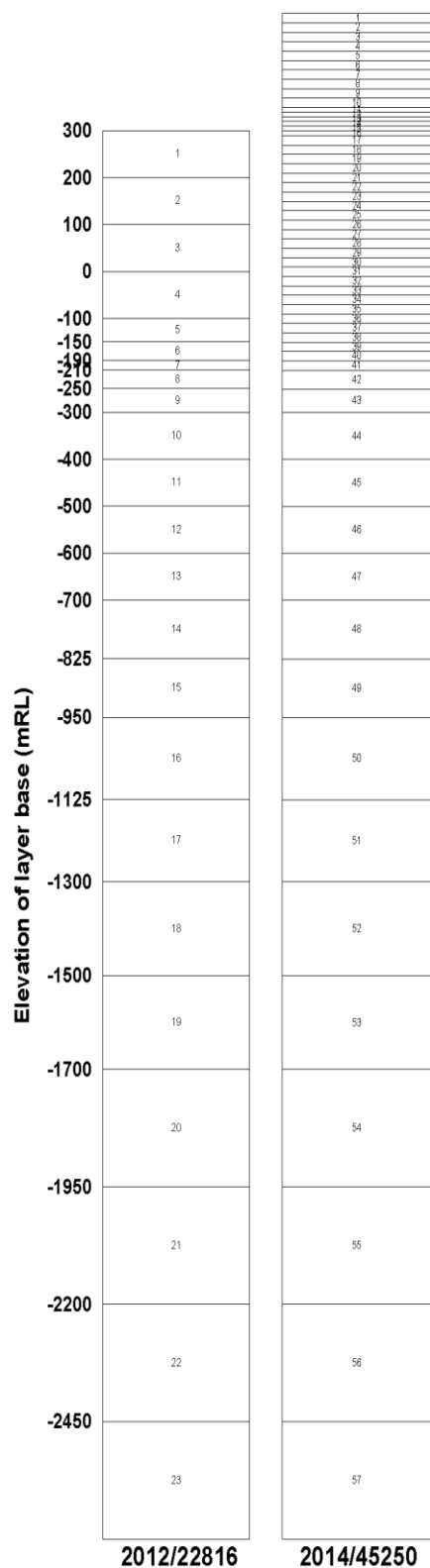


Figure 3: Layer structure for Models 2012 (left) and 2014 (right)

With this model the unsaturated zone, between the water table and ground surface contains water vapour and CO₂ (not air) which is a reasonable approximation and one that

is necessary because an equation of state for water and all components of air is not available with TOUGH2.

At the bottom boundary of the model mass, heat and CO₂ are injected. These deep inflows were varied as part of the natural state calibration process. A background conductive heat flux of 120mW/m² is used. This is considered to be a reasonable value for zones close to convective upflows in the Taupo Volcanic Zone. The heat flux is increased in blocks close to the main reservoir, representing the greater heat flow anomaly associated with Ohaaki. The mass inflow at the bottom of the model represents the upwelling from the part of the convective plume which has not been captured within the model (i.e. from convective circulation below the base of the model). The CO₂ is injected at an average mass fraction of 1.1%, representative of the amount found in wells at Ohaaki. A summary of the total heat, mass and CO₂ injected into the base of the model is shown in Table 2. A heat input of 123MW is applied to the model, which is close to the natural heat flow of around 100MW suggested by Allis (1980), but as there is large uncertainty in this value, the model heat flow is reasonable.

Table 2: Total flow into the base of the model.

	Enthalpy (kJ/kg)	Temperature °C	Mass/Heat flow
Mass (kg/s)	1430	314.85	72.2
Conductive heat (MW)	-	-	39.6
CO ₂ (kg/s)	1430	314.85	0.80
Convective heat (MW)			98.9
Total heat (MW)			122.6

In Table 2 the total has a background heat flow of 70mW/m² removed.

There are two aspects to determining the horizontal extent of the model. Firstly, the horizontal area of the model is large enough to capture most of the hydrothermal convective regime at Ohaaki and so for natural state modelling all side boundaries can be treated as closed.

The second factor to consider with respect to model boundaries is that reservoir behaviour during history matching and future scenario simulations should not be subject to boundary effects. Ohaaki has a large boiling zone and high CO₂ content. The pressure changes in the reservoir are buffered by the expansion and contraction of the boiling zone, and hence do not spread to the edges of the model. Thus, no-flow, closed boundaries are used for all simulations, and checks show that the pressures near the boundaries of the model do not change.

3.3 Geological model

Recent collaboration with ARANZ and GNS Science and the use of the LEAPFROG geological modelling software (Alcaraz *et al.*, 2011, 2012) has introduced an automated way of extracting the geological model rock-types and applying them to the elements in our TOUGH2 model. New

TOUGH2 simulation input files can be created within the software and results can be visualised Newson *et al.* (2012).

One of the significant improvements in moving on from Model 2012 was the use of the LEAPFROG model to review and update the rock-type assignment and permeability structure for Model 2014 so that it closely matches the geological model. Within the TOUGH2 model we still allow some subdivision of the major rock-types to allow for heterogeneity e.g. different permeability arising from different levels of fracturing. Such subdivision of reservoir properties is required to get a good match of model behaviour to the natural state and production history data (discussed below).

4. NATURAL STATE MODEL

4.1 Implementation

The first stage of model development is natural state modelling (O'Sullivan *et al.*, 2001). This is aimed at reproducing the conditions of the reservoir before any production or drilling occurred. The model is run until the reservoir is in a steady state with pressures and temperatures no longer changing. Permeability and deep inflows are then adjusted iteratively until the model matches the observed down-hole temperatures. For early wells, this is the pre-production 'natural state' condition of the system.

4.2 Natural state temperatures

A complete set of results for Model 2012 for downhole temperatures was given by O'Sullivan and Clearwater (2013). Two typical plots, one for the West bank and one for the East Bank are presented here, comparing the results for Models 2012 and 2014. Note that for wells that were drilled recently the model results are taken from the production history simulations at the appropriate time rather than the pre-exploitation natural state model.

A comparison of the two sets of model results with data for a well on the West Bank is shown in Figure 4. For this well there is a temperature inversion at 0mRL which is due to cold groundwater in the Ohaaki Rhyolite formation. Early wells drilled on the West Bank feed from the intermediate reservoir, at about -100 to -900 m RL, and newer West Bank wells feed from levels between -1300 and -2100 mRL. Both models show a good match to the field temperatures at these elevations. In this case the results for Model 2014 the shallow temperature maximum at 100 mRL and the cold inflow at -1200 mRL require further calibration.

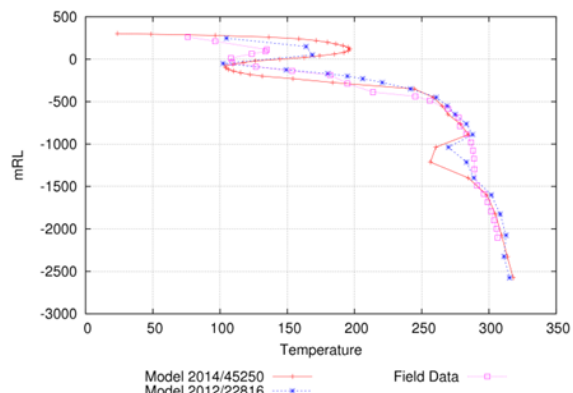


Figure 4: Temperature profiles for a typical West Bank well.

Results for both models for a typical well on the East Bank are shown in Figure 5. The two sets of results are very similar and both models are a good match to the data.

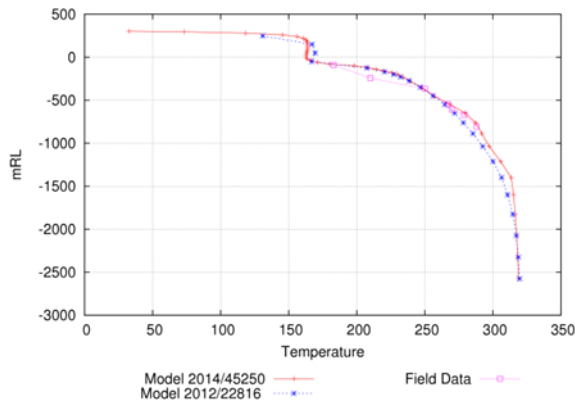


Figure 5: Temperature profiles for a typical East Bank well.

5. PRODUCTION HISTORY MODELLING

5.1 Implementation

To simulate the production history, the recorded production and injection rates for each well have to be assigned to the correct block in the model. This apparently simple process turned out to be quite complicated for Ohaaki. Because of the difficulty in accurately measuring two-phase flow at the time of the commissioning the OGPP production data from individual wells at Ohaaki is not available. Instead, the total mass flow and average production enthalpy data for the group of wells connected to each separator are recorded. For each well the operating well head pressure is regularly recorded, along with the status of the well (whether it is on production, on bleed, closed, reinjecting, etc.). Thus the number of days per week that the well is on production is recorded, and therefore the proportion of each week that each well is open can be determined.

Individual wells are output tested every six months, and these tests provide characteristic curves for each well from which it is possible to derive a flowrate given the measured wellhead pressure. These tests also provide information on the proportion of total flow each well is providing to the separator. These proportions are assumed to remain constant from one output test to the next and are used to apportion the separator mass flow to the individual wells. Account is also taken of when particular wells are out of service. These calculated flows for the individual wells are then put into the TOUGH2 data file for the production history simulation.

For multi-feed wells the process is even more complicated and production is further broken down further by assigning a proportion of the total flow rate to each feed. These proportions are held constant with time.

Neither of these two procedures for assigning mass flows to individual wells and to each feed-zone for each well is entirely satisfactory. The well characteristic curves and proportion of the contribution from each well to the separator vary from one output test to the next and the

enthalpy response of the model is quite sensitive to flow rate.

Assembling the historical injection data was a much simpler and more accurate process as continuous injection rates for each injection well have been measured. At Ohaaki 100% of the separated geothermal water (SGW) is reinjected, and 30% of the condensate is reinjected while the rest is lost to atmosphere through the large natural draft cooling tower.

For the production history simulation the period simulated is from 1966 to 2012. This encompasses early well testing, a recovery period and the operation of the OGPP from 1988 onwards.

Calibration of the production history model is performed by comparing pressure, enthalpy and CO₂ histories. Adjustments to porosities, permeabilities and the deep upflows are made as required. Pressure data are available from several monitoring wells throughout the field, and 6-monthly output tests provide pressures, production enthalpies and CO₂ mass fractions for all the production wells.

Of the surface features at Ohaaki, only the Ohaaki pool is represented in the reservoir model. This is the only feature which has a significant mass flow, with other features having diffuse heat and mass discharge (i.e. warm and steaming ground). The Ohaaki pool at natural state discharged at a constant rate of approximately 10kg/s. After early well testing and production, discharge from this pool fluctuated and then ceased. The bottom of the pool has since been cemented, blocking natural fluid flow, and the pool is now filled with SGW. In the natural state, the Ohaaki pool is represented in the model by the extraction of 10kg/s at the depth in the reservoir from which the fluid is thought to have come. For Model 2012 this was continued for the production history simulations but for Model 2014 the mass flow to the Ohaaki pool is allowed to vary with time by using a well on deliverability to represent this flow. Thus there is a variable mass flow for the well testing, recovery and production period, up until the base of the pool was sealed off in 1989. Switching the “well” on to deliverability allows for a better representation of observed flow to the pool, and hence provides more information about the interaction between the pool and nearby wells. The productivity index chosen for the well corresponds to the natural state mass flow of 10kg/s.

Prior to 1997 steam from Ohaaki was supplied for timber drying from a well separate from the production field. The timber drying facility required a specified amount and a specified dryness fraction. This was applied using a POWR generator (a new well-type created in AUTOUGH2). The POWR generator type allows a well to produce enough mass to satisfy a target steam flow rate, given a specified separator pressure, cut-off pressure, and minimum steam quality. In 1998 the well providing steam to the timber plant was connected to the production system, and no excess steam was available for the timber drying plant. Instead, some of the SGW, instead of being re-injected, was supplied for timber drying.

5.2 Production history results

A complete set of results for the production history version of Model 2012 are given in O’Sullivan and Clearwater

(2013). A few typical plots are given below with results for Model 2014 added for comparison.

Some of the plots (Figures 8-10) show that an improved match to the shallow pressure response has been achieved with Model 2014, although calibration has not yet finished and more improvement may be achieved.

Pressure

The *Reservoir Engineering* section of Carey *et al.*, 2013 identifies the following five main hydrological units:

- (i) **Groundwater**: Aquifers from the surface down to 100m depth, generally lying above the Huka Formation.
- (ii) **Inner Rhyolite**: This aquifer is hosted in the Ohaaki Rhyolite at depths of 100-400m and lies partly over the West Bank production areas.
- (iii) **Intermediate Aquifer**: The original high temperature production reservoir at depths of 400-1200m, generally hosted in Waiora Formation and Rautawiri Breccia.
- (iv) **Deep Aquifer**: The high temperature productive area on the West bank below depths of 1500m, hosted in Tahorakuri Formation.
- (v) **Outfield, Outer Rhyolite**: Generally intermediate depth aquifers hosted in cool rhyolite bodies at depths of 400 to 800m and hydrologically isolated from the hot reservoir.

Figure 6 is a visual description of these aquifer units, overlain by the grid structure of Model 2012. The three productive reservoir pressure regimes used to represent the reservoir modelling results (shallow, intermediate and deep) are also shown.

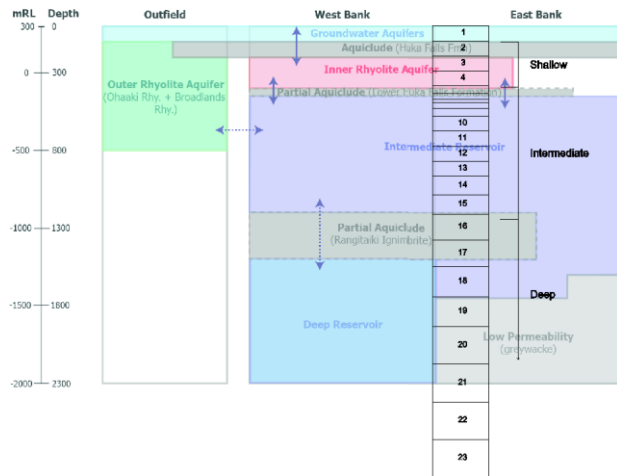


Figure 6: The hydrologic zones identified within the Ohaaki reservoir and surrounding aquifers (Carey *et al.*, 2013), compared to the model grid structure.

This classification of the aquifers at Ohaaki is used in the discussion of model results for pressures presented in this section.

The model pressures during the well testing and production period show a good match to the field data, especially for most new deeper wells on the West Bank. The results for the pressure on the East Bank at the centre of layer 11 (-450mRL), are shown in Figure 7.

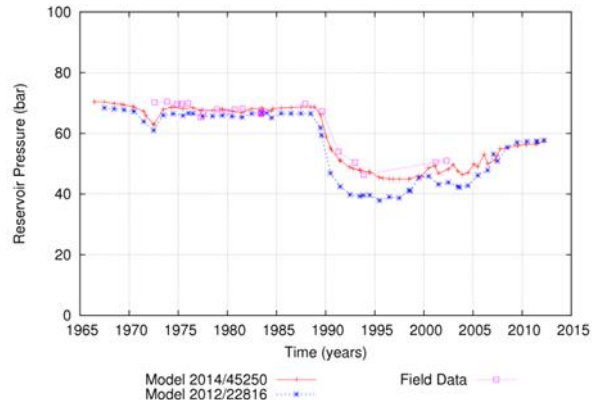


Figure 7: Pressure vs. Time for a shallow East Bank well.

Model 2014 follows the pressure drawdown very well, whereas Model 2012 shows the correct trend but with a little too much drawdown.

The pressure drawdown histories from two deep feeding West Bank wells are shown in Figure 8. The model results in this plot are taken from layer 19 (1900m deep). There are two wells that feed from this column at different depths. The shallower well operated during the early well testing period and production period until 1995, and the deeper well was drilled and started producing in 2007. The models show a good match to the data for the earlier period, and approximately the correct amount of drawdown at 2007. The very recent pressure drawdown in the models qualitatively matches the observed rapid decline but further calibration of the permeability in the deep zone is required to improve the match.

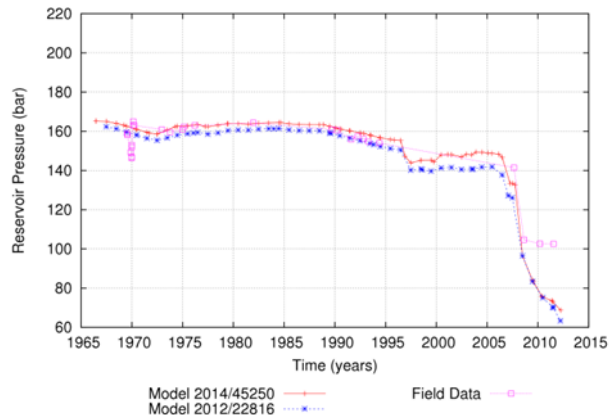


Figure 8: Pressure vs. Time for a deep West Bank well.

Figure 9 shows a plot of pressures in the Inner Rhyolite aquifer (elevation 20 mRL) on the West Bank. The results for Model 2014 are significantly better than for Model 2012 but the large pressure drop between 1995 and 2005 is not being captured by the model. Evidently this part of the model is too well connected, either horizontally or vertically, to zones affected by a local reduction of production or by reinjection.

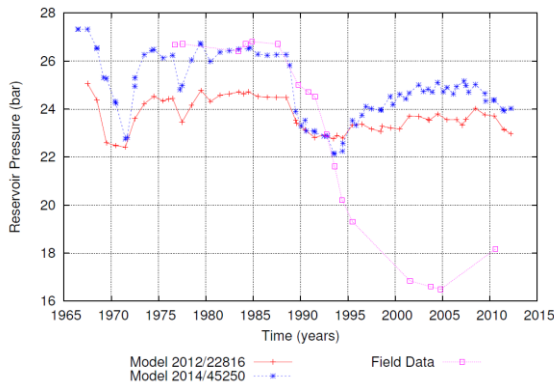


Figure 9: Pressure vs. Time for a well in the Inner Rhyolite, West Bank.

Figure 10 shows pressures from a well in the Intermediate Aquifer located near the centre of the subsidence anomaly. Again the results for Model 2014 are significantly better than for Model 2012.

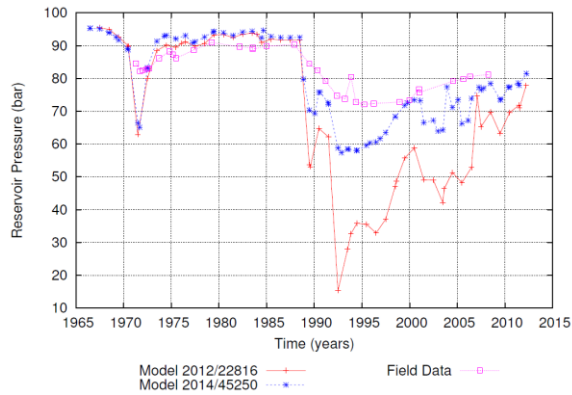


Figure 10: Pressure vs. Time for BR20 in the Intermediate Aquifer, West Bank.

Enthalpy

In general the well-by-well performance of the model match is reasonable. However, further calibration is required for some areas where not enough boiling is occurring – especially over a period over 1990 to 2000, as shown in Figure 11. The results from the two models are very similar.

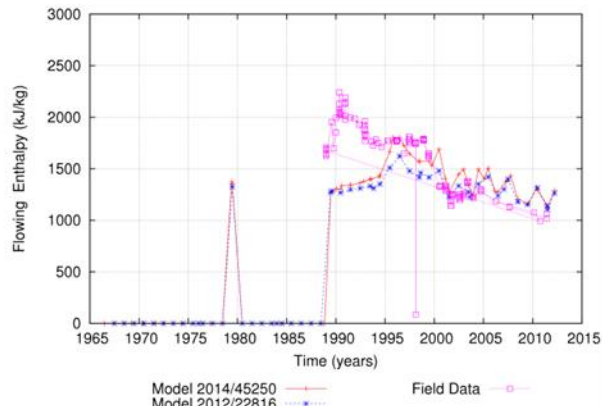


Figure 11: Enthalpy results for a typical East Bank well.

Enthalpy data is quite variable from well to well – the East Bank wells tend to have an initial increase in enthalpy followed by a slow decline, whereas the West Bank wells start out at a lower enthalpy which stays constant or increases over time.

The average enthalpy for one of the West Bank separators is shown in Figure 12. The results for both models are very similar but there is a small improvement for Model 2014 between 1990 and 2000.

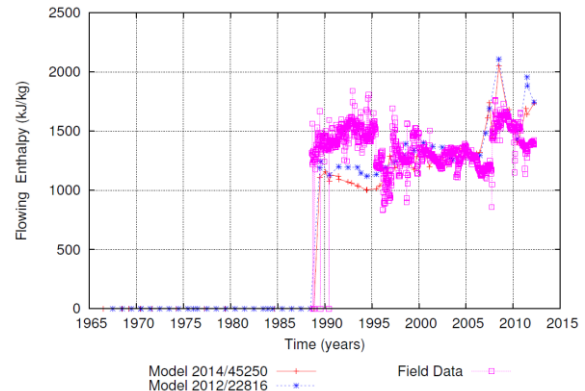


Figure 12: Separator enthalpy results

CO_2 mass fraction

For both models the results for carbon dioxide content versus time are of mixed quality. For some wells the model match is very poor, but often this is associated with a mismatch in enthalpy which can be improved by further calibration. For other wells, the match is good, as shown in Figure 13. Overall trends and magnitudes averaged field wide are reasonable. In this case the early peak at 1990 is a worse fit for Model 2014 but this model gives a better fit from 1995 onwards.

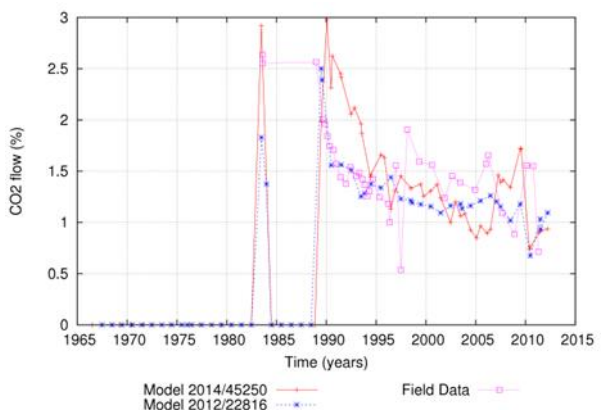


Figure 13: CO_2 vs. Time for a typical West Bank well.

Injection

So far there has been no observed effect of injection on production and therefore a single porosity model is used. The model results show the injected fluid spreading away from the production area.

Twenty-seven tracer tests conducted between 1974 and 1994 (McCabe *et al.*, 1995) showed very little connection between the injection and production wells and the tracer

test conducted in 1999 (Rose *et al.*, 2000) showed only a small amount of return to the two nearest production wells with most of the tracer heading away from the production zone.

6. FUTURE SCENARIOS

Once a satisfactory match to the available data (natural state and production history) is obtained the model can be used to simulate the future behaviour of the geothermal system in response to various production and reinjection scenarios.

The initial values of pressure and temperature for the future scenario simulations are taken from the final values in the production history simulation. In the future scenario simulations, the wells are operated in “deliverability” mode. In this mode, as in real life, the flow rate depends on the feed block pressure and as the block pressure declines, the flow rate declines. This assumes that the wells remain in good condition and thus the model may produce an optimistic result if wellbore effects such as calcite scaling become important.

A number of features have been added to the AUTOUGH2 simulator to assist with scenario modelling (Yeh *et al.*, 2012). Make-up wells are automatically added when either the total mass flow or the total steam flow from a set of wells falls below a pre-set target. Reinjection can be made proportional to the total separated water flow or the total condensate flow.

6.1 Description of Scenarios

Six different future scenarios were simulated with Model 2012. These simulations have not yet been repeated with Model 2014. However, we present the results from the earlier model here as they have not previously been published apart from in the report for the resource consent application (O’Sullivan and Clearwater, 2013). These scenarios were provided by CEL and are outlined in the System Management Plan (Contact Energy Ltd., 2013). The purpose of these scenarios was to observe the effect of the proposed 35 year term of consent on the Ohaaki system. The scenarios are:

- Scenario 1A. Allow existing production wells to run on deliverability until 31 October 2013. A take of 35,000 t/day of mass is to then be maintained using existing wells plus make-up wells.
- Scenario 1B. Allow existing production wells to run on deliverability until 31 October 2013. A take of 40,000 t/day of mass is to then be maintained using existing wells plus make-up wells. This is the consent application scenario.
- Scenario 1C. Allow existing production wells to run on deliverability until 31 October 2013. A take of 45,000 t/day of mass is to then be maintained using existing wells plus make-up wells.
- Scenario 1D. Allow existing production wells to run on deliverability until 31 October 2013. A take of 9,600 t/day of steam, sufficient to run one intermediate pressure turbine at full load, is to then be maintained for as long as possible using existing wells plus make-up wells. If the reservoir can no longer maintain this steam take, instead maintain a maximum take of 40,000 t/day of mass, using existing wells plus make-up wells.
- Scenario 1E. Allow existing production wells to run on deliverability until 31 October 2013 when all production and reinjection is ceased. This scenario is modelled in

order to show the effect of the proposed consent not being granted.

- Scenario 1F. Allow existing production wells to run on deliverability until 31 October 2013. A take of 40,000 t/day of mass is to then be maintained using existing wells plus make-up wells. Continue until 31 October 2048 when all production and reinjection is ceased. This scenario is included to observe the effect on the system if production ceases after the 35 year consent term.

In all cases, except for the shut-down parts of Scenario 1E and 1F, reinjection is included, with 30% injected in the north, 50% in the west, and 20% in the east. This reinjection strategy is similar to that currently implemented for the OGGP. No make-up reinjection wells were included.

The initial conditions for the predictive modelling are the final conditions obtained at the end of the production history run. Existing production wells are used, with additional make-up wells added as required to meet the target total mass or steam flows throughout the simulation time. Carrying on the simulations until 2060, demonstrates the effect of continuing production beyond the proposed consent period of 35 years.

6.2 Determination of deliverability parameters

For the future scenario simulation all wells are run on deliverability, and this means there are two parameters required for each well – a cut off pressure and a productivity index (PI). The cut off pressures vary with depth and enthalpy, and were calculated by CEL reservoir engineers. For each feed-zone depth a table of enthalpy vs. cut-off pressure was provided, as outlined in the System Management Plan (Contact Energy Ltd., 2013).

The PI for each production well is calculated in the the following manner. After one step of length one second the mass flow rate is compared to that at the end of the production run and then the PI is adjusted so that the mass flows at the start of the new simulation match those at the end of the production history run. This is a simple calculation as the mass flow is proportional to productivity index. The calculated PI is then used for rest of the simulation.

6.4 Make-up wells

In the model the make-up wells are distributed approximately uniformly across the designated zones. For each scenario, make-up wells are added once the overall mass take drops below the scenario target. The productivity index used for each make-up well is 1.23E-12. This value was calculated as an average of all the production wells prior to 2007, before the latest large producers were included in the production history. Hence this value is slightly lower than the average PI of all the production wells included in the scenarios, thus giving a conservative performance of the model.

For the make-up wells 80% were located on the West bank and the remaining 20% on the East bank, as specified by CEL. Figure 14 is a map displaying these locations.

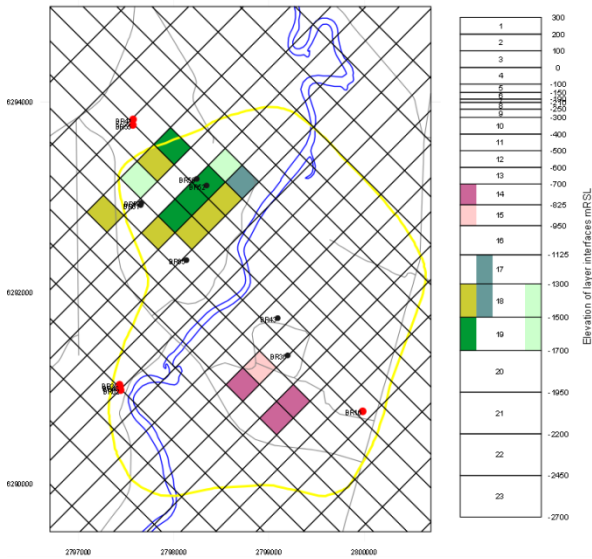


Figure 14: Location of production and make-up wells. The black dots represent the wellhead location of production wells used in the scenarios, and red dots reinjection wells. The coloured squares represent the make-up well locations with their corresponding feedzone elevations.

7. RESULTS OF FUTURE SCENARIOS

A complete set of results for Model 2012 was presented by O'Sullivan and Clearwater (2013). A brief summary is included here.

7.1 Mass Flows

The total mass flows for each scenario are shown in Figure 15. The plot shows that for Scenarios 1A and 1B the required mass takes are easily reached over the whole time period simulated. For Scenario 1C the mass target can be met for the first 5 years, but then cannot be maintained, even with all 20 make-up wells, and drops to ~43,000 t/day.

In the various scenarios there is complex interaction between total mass flow and total steam flow. A higher mass flow leads to a larger pressure drop, more boiling and a higher production enthalpy and therefore a proportionally higher steam flow.

The mass flow for Scenario 1D is not fixed as the mass take varies depending on the enthalpy of the fluid produced. The higher the enthalpy the more easily the steam target is achieved, with a smaller mass take required. Figure 15 shows that Scenario 1D needs an increasing mass flow to maintain the flow of 9,600 t/day of steam, but it is never constrained by the cap of 40,000 t/day of mass, reaching a maximum mass flow of only ~37,500 t/day.

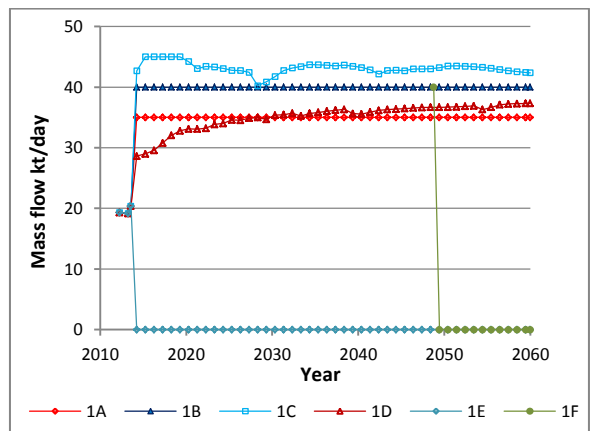


Figure 15: Total mass flows for the future scenarios

There is a large increase in mass flow at the end of 2013 as the make-up wells are required to be opened up to meet the specified fixed mass takes. For Scenario 1A (35,000 t/day), after this initial increase, the mass flow rate is constant throughout the rest of the scenario, with approximately 24,000 t/day coming from the West Bank wells. However, for Scenarios 1B and 1C (40,000 t/day and 45,000 t/day respectively), the mass flow from the West Bank peaks at ~30,000 t/day and then drops back to approximately 25-27,000 t/day from 2030 onwards. A much smaller amount of mass is taken from the East Bank: between 10-16,000 t/day for all scenarios.

7.2 Steam Flows

The steam flow is based on a separator pressure of 5 bar. This is only indicative, as the actual steam flow will depend on the separator configuration for each group of wells. The total steam flow for each scenario is shown in Figure 16. Scenarios 1A and 1B show similar steam flow trends, namely an initial increase then a steady decline which tapers off by about 2040.. For Scenario 1C the addition of make-up wells gives a large initial increase in steam flow as the reservoir tries to make up the 45,000 t/day of mass required, but the peak steam rate of 17,500 t/day cannot be maintained as the reservoir slowly cools after 2020 and the steam flow declines, reaching a similar steam flow to that for Scenario 1B by 2060.

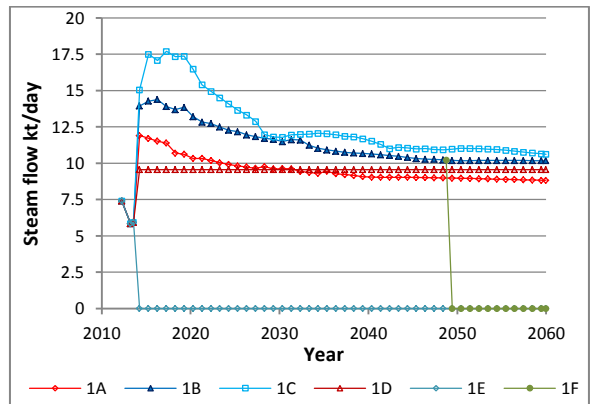


Figure 16: Steam flows for the future scenarios

Scenario 1D required the steam flow to be fixed at 9,600 t/day for as long as possible. Figure 16 shows that the reservoir can supply this target steam flow for the whole time period simulated.

7.3 Enthalpy

Average production enthalpies for each scenario are shown in Figure 17. These plots confirm the gradual cooling of the reservoir for each of the scenarios. The make-up wells give an initial increase of enthalpy for most scenarios; however all scenarios have a final average enthalpy stabilising from about 2050 onwards at a value ranging from 1171 – 1182 kJ/kg.

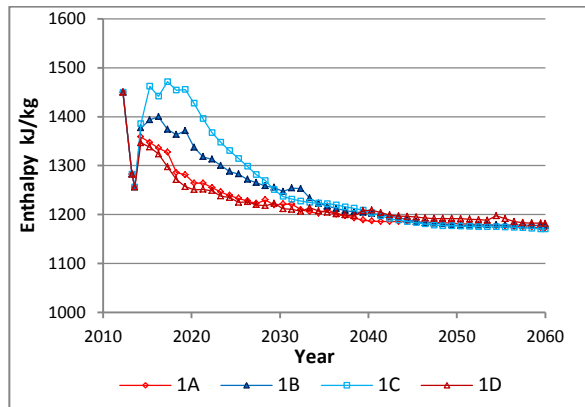


Figure 17: Average production enthalpy for the future scenarios

7.4 Pressures

Figure 18 shows the pressure history for the shallow reservoir on the West Bank (50 mRL). For Scenarios 1A-D the shallow pressure slowly increases over the 48 years simulated, the total increase being about 1 bar. Scenarios 1E and 1F show a recovery of pressure that will be discussed further below.

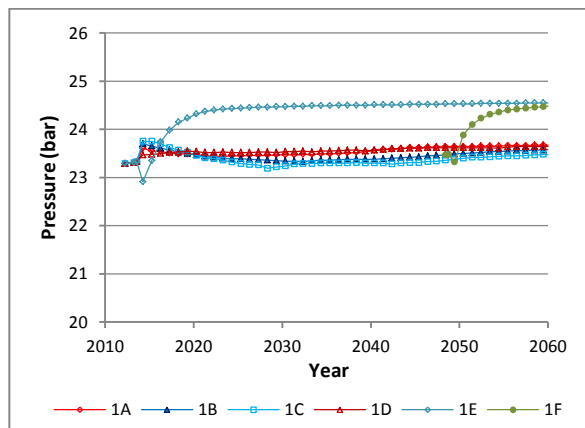


Figure 18: Shallow pressures on the West bank

Figure 19 shows the pressure history for the deep reservoir (-1825 mRL) on the West Bank. There is a large early pressure drop (up to ~30 bar for Scenario 1C) for Scenarios 1B and 1C, which ceases by ~2035, and is followed by a slow rise in pressure, interpreted to be the effect of nearby injection wells. Scenarios 1A and 1D exhibit a smaller early pressure decline, and from 2040 onwards the pressures remain almost constant.

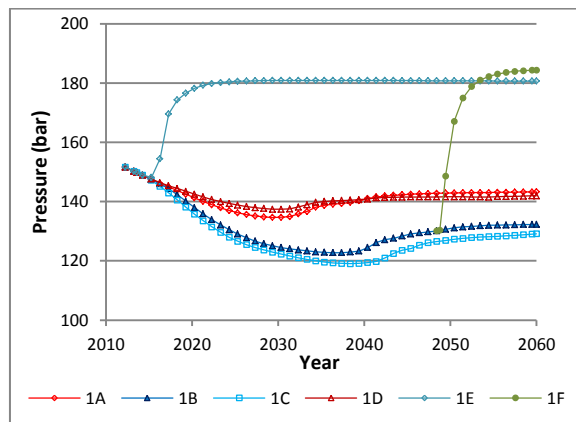


Figure 19: Deep pressures on the West Bank

7.5 Temperatures

Figure 20 shows temperature history for the deep reservoir. The temperature decline here is very small, at ~3°C or less for all scenarios.

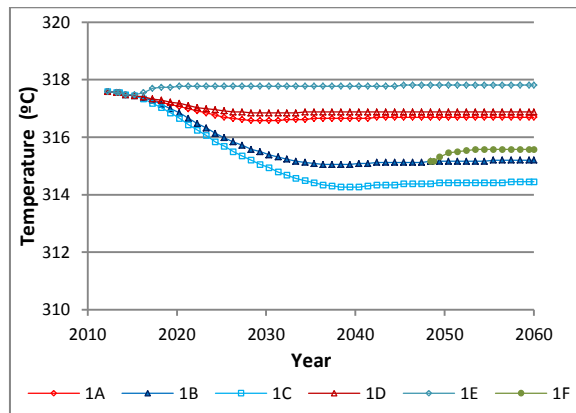


Figure 20: Deep temperatures on West Bank

7.5 Pressure and Temperature Recovery

Figure 21 shows a plot of pressures over the period 1968 to 2060, covering the well testing period, recovery period, production history and future scenarios. The aim of these plots is to show the recovery of the Ohaaki reservoir for Scenario 1E (shut-down in 2013) and 1F (shutdown in 2048). Results are shown for the West bank at intermediate depths.

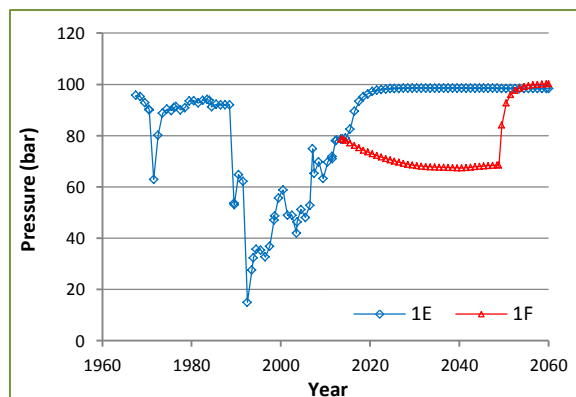


Figure 21: Pressure recovery after shut-down

For Scenario 1E, pressure recovers very rapidly once production ceases in 2013 and stabilises by 2030. The resulting pressure is slightly higher than the natural state value (by up to about 2 bar) which is to be expected as the temperature has not returned to the natural state (see next paragraph), and so the reservoir fluid in 2060 is cooler, and hence more dense than the pre-production state. It will also have a lower gas saturation.

For the 2048 shut-down scenario (1F), the response is much the same. The resulting pressures are slightly higher than after the 2013 shut down (Scenario 1E) pressures.

Figure 22 shows the temperature histories for Scenarios 1E and 1F (for the same block as the pressure plot), from natural state through to 2060. At the intermediate level shown, the natural state temperature is still ~30°C lower than natural state.

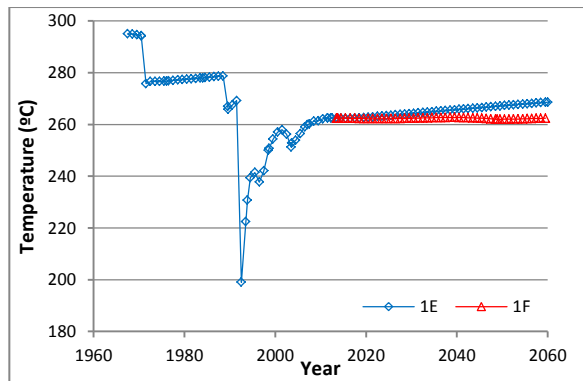


Figure 22. Temperature recovery after shut-down

8. CONCLUSIONS

8.1 Model 2012

This is the model presented in evidence at the 2013 hearing on the re-consenting of the Ohaaki power project. The model shows a good match to the downhole temperatures at pre-production and later times. The production history simulations give a good match to measured enthalpies and pressure changes, and a reasonable match to changes in CO₂ content.

The deep zone on the West Bank of the Waikato River is a part of the model for which there is a relatively short production history and therefore a limited amount of past data with which to calibrate this part of the model. However for the existing deep western wells which are included in the future scenarios the model results match the past enthalpy behaviour very well, and pressure behaviour is matched reasonably well.

Some other conclusions from the future scenario simulations are:

- A take of up to 40,000 t/day of mass (Scenario 1B) can be maintained over the modelling period (2013 to 2060). This demonstrates that the system can sustain 40,000 t/day of production up to and beyond the 35 year application period. All of the make-up wells are not required, and the average production enthalpy declines very slowly from 2050 onwards. For Scenario 1B the deep pressures on the West Bank decline by up to 25 bar at around 2037, but then

recover to a 20 bar decline by 2060. The shallow pressure decline (at a depth of 350m) is much less at ~3 bar, recovering to less than 1 bar. By 2060 the production enthalpy has stabilised at 1179 kJ/kg and temperatures in the deep reservoir at -1825 mRL (metres relative to sea level) are still high (over 300°C). Hence there is a lot of useful heat still available in the reservoir.

- A take of 45,000 t/day (Scenario 1C) cannot be maintained over the modelling period as there are not enough make-up wells to sustain that mass flow rate.
- The main difference between Scenarios 1A, 1B and 1C (with mass takes of 35kt/day, 40kt/day and 45kt/day, respectively) is in the deep pressure behaviour on the West Bank, with maximum declines of 8.8, 20.1 and 23.3 bar, respectively. Other results, for instance shallow pressures and temperatures at all depths, differ less between the scenarios.

8.2 Model 2014

This is the latest version of the model, with a fine shallow layer structure that includes the very shallow unsaturated zone Model 2014 is still undergoing calibration but the results presented here show that it is already matching the natural state temperatures and the production history data as well as or better than Model 2012. Some of the pressure vs time results (see Figures 8 and 9) are significantly better with Model 2014.

ACKNOWLEDGEMENTS

We thank Contact Energy Limited for permission to publish this paper and financial support of our modelling study of Ohaaki.

REFERENCES

- Alcaraz, S., Lane, R., Spragg, K., Milicich, S., Sepulveda, F. and Bignall, G.: 3D Geological Modelling Using New Leapfrog Geothermal Software. *Proc. 36th Workshop on Geothermal Reservoir Engineering*, Stanford University, Stanford, California, (2011).
- Alcaraz, S., Rattenbury, M., Soengkono, S., Bignall, G. and Lane, R.: A 3D Multi-Disciplinary Interpretation of the Basement of the Taupo Volcanic Zone, New Zealand. *Proc. 37th Workshop on Geothermal Reservoir Engineering*, Stanford University, Stanford, California, (2012).
- Blakeley, M.R., O'Sullivan, M.J. and Bodvarsson, G.S.: A simple model of the Ohaaki Geothermal Reservoir, *Proc. 5th New Zealand Geothermal Workshop*, Auckland, New Zealand, pp. 11-16. (1983).
- Carey, B., Alcaraz, S., Soengkono, S., Mroczek, E., Bixley, P., Rae, A., Lewis, B., Reeves, R. and Bromley, C.: *Ohaaki Geothermal Power Plant. Project Reference Report: Geoscientific and Reservoir Engineering Review*. GNS Science Consultancy Report 2011/273, 236p., (also Appendix C to Part B, the Assessment of Environmental Effects Report, submitted by Contact Energy to the Waikato Regional Council in support of an application for Resource Consents for the Ohaaki Geothermal Power Plant). (2013).
- Clearwater, E. K., Brockbank, K., and O'Sullivan, M. J.: An update on modelling the Ohaaki geothermal system.

- Proc. 33rd New Zealand Geothermal Workshop.*
Auckland. New Zealand. (2011).
- Clotworthy, A., Lovelock, B. and Carey, B.: Operational History of the Ohaaki Geothermal Field, New Zealand., *Proc. World Geothermal Congress*, Florence, Italy, pp. 1797-1802. (1995).
- Contact Energy Ltd: *Ohaaki Geothermal Power Plant. Draft System Management Plan for the Ohaaki Geothermal System, April 2013*. Document submitted by Contact Energy to the Waikato Regional Council in support of an application for Resource Consents for the Ohaaki Geothermal Power Plant. (2013).
- Hedenqvist, J.W.: The thermal and geochemical structure of the Broadlands-Ohaaki geothermal system, New Zealand. *Geothermics*, 19(2), pp. 151-185. (1990).
- Lee, S. and Bacon, L.: Operational History of the Ohaaki Geothermal Field, New Zealand. *Proc. World Geothermal Congress*, Kyushu-Tohoku, Japan, 2000, pp. 3211-3216. (2000).
- McCabe, W.J., Clotworthy, A.W. and Morris, C.: Results of repeat tracer tests at Ohaaki, NZ. *Proc. 17th New Zealand Geothermal Workshop*. Auckland. New Zealand. (1995).
- Newson, J.A. and M. J. O'Sullivan, M.J.: Modelling the Ohaaki Geothermal System. *Proc. 26th Workshop on Geothermal Reservoir Engineering*, Stanford University, Stanford, California, pp. 186-192. (2001).
- O'Sullivan, M.J. and Clearwater, E.: *Ohaaki Geothermal Power Plant Project Reference Report: Reservoir Modelling*. Uniservices Report, 169 p., (also Appendix D to Part B, the Assessment of Environmental Effects Report, submitted by Contact Energy to the Waikato Regional Council in support of an application for Resource Consents for the Ohaaki Geothermal Power Plant.). (2013).
- O'Sullivan, M.J., Pruess, K. and Lippmann, M.J.: State of the art of geothermal reservoir simulation. *Geothermics*, 30, 395-429, (2001).
- Rae, A.J., Rosenberg, M.D., G. Bignall, G., Kilgour, G.N. and Milicich, S.: Geological Results of Production Well Drilling in the Western Steamfield, Ohaaki Geothermal System: 2005-2007. *Proc. 29th New Zealand Geothermal Workshop*, Auckland, New Zealand. (2007).
- Risk, G.F., MacDonald, W.J.P. and Dawson, G.D.: D.C. resistivity surveys of the Broadlands geothermal region, New Zealand. *Geothermics*, 2(1), pp. 2787-294. (1970).
- Rose, P., Benoit, R., Lee, S.G., Bagus Tandia, B. and Kilbourn, P.: Testing the naphthalene sulfonates as geothermal tracers at Dixie Valley, Ohaaki, and Awibengkok. *Proc. 25th Workshop on Geothermal Reservoir Engineering*. Stanford University, Stanford, California, January 24-26 (2000).
- Wood, C.P., Brathwaite, R.L. and Rosenberg, M.D.: Basement Structure, Lithology and Permeability at Kawerau and Ohaaki Geothermal Fields, New Zealand. *Geothermics*, 30, 461-481, (2001).
- Yeh, A., Croucher, A. E. and O'Sullivan, M.J.: Recent developments in the AUTOUGH2 simulator. *Proc. TOUGH Symposium 2012*, Berkeley, California, USA. (2012).
- Zarrouk, S.J. and O'Sullivan, M.J.: Recent Computer Modelling of the Ohaaki Geothermal System. *Proc. 28th New Zealand Geothermal Workshop*, Auckland, New Zealand. (2006).